Scientific Report

SOURCE DATA | TRANSPARENT PROCESS

EMBO reports

Calcineurin promotes APC/C activation at meiotic exit by acting on both XErp1 and Cdc20

Andreas Heim[1,2], Thomas Tischer[3] & Thomas U Mayer[1,2,*]

Abstract

Vertebrate oocytes await fertilization arrested at metaphase of the second meiotic division. Fertilization triggers a transient calcium wave, which induces the activation of the anaphase-promoting complex/cyclosome (APC/C) and its co-activator Cdc20 resulting in the destruction of cyclin B and hence meiotic exit. Two calcium-dependent enzymes are implicated in fertilization-induced APC/C^{Cdc20} activation: calcium-/calmodulin-dependent kinase type II (CaMKII) and calcineurin (CaN). While the role of CaMKII in targeting the APC/C inhibitor XErp1/Emi2 for destruction is well-established, it remained elusive how CaN affects APC/C^{Cdc20} activation. Here, we discover that CaN contributes to APC/C^{Cdc20} activation in *Xenopus laevis* oocytes by two independent but interrelated mechanisms. First, it facilitates the degradation of XErp1 by dephosphorylating it at a site that is part of a phosphorylation-dependent recruiting motif for PP2A-B′56, which antagonizes inhibitory phosphorylation of XErp1. Second, it dephosphorylates Cdc20 at an inhibitory site, thereby supporting its APC/C-activating function. Thus, our comprehensive analysis reveals that CaN contributes to timely APC/C activation at fertilization by both negatively regulating the APC/C inhibitory activity of XErp1 and positively regulating the APC/C-activating function of Cdc20.

Keywords APC/C; Calcineurin; Cdc20; Meiosis; *Xenopus laevis*; XErp1
Subject Categories Cell Cycle; Post-translational Modifications, Proteolysis & Proteomics; Signal Transduction
DOI 10.15252/embr.201846433 | Received 16 May 2018 | Revised 5 October 2018 | Accepted 5 October 2018 | Published online 29 October 2018
EMBO Reports (2018) 19: e46433

Introduction

In vertebrates, fertilizable oocytes are arrested at metaphase of the second meiotic division (MII) in a state with active Cdk1/cyclin B and inactive APC/C^{Cdc20} [1,2]. This MII arrest is mediated by a biochemical activity termed cytostatic factor (CSF) composed of the APC/C inhibitor XErp1/Emi2 and factors mediating its activation [3–6]. XErp1/Emi2 binds directly to the APC/C and inhibits it by multiple mechanisms [7–9]. In *Xenopus* oocytes, activation of XErp1 requires its phosphorylation by the 90-kDa ribosomal protein S6 kinase (p90^{RSK}), the downstream kinase of the c-Mos-/mitogen-activated protein kinase (MAPK) pathway [5,6]. Upon phosphorylation of XErp1 by p90^{RSK}, protein phosphatase PP2A in complex with the regulatory B′56 subunit binds to XErp1 and protects it from inhibitory phosphorylation by Cdk1/cyclin B and other kinases [10,11]. In *Xenopus* oocytes, the transient rise in calcium levels associated with fertilization causes the activation of the kinase CaMKII and the phosphatase calcineurin (CaN, also called PP2B) [12–14]. The role of CaMKII in meiotic exit is well-established and seems to be highly conserved across species [15]. Activated CaMKII phosphorylates XErp1 at Thr195 and thereby creates a docking site for polo-like kinase 1 (Plx1) [16]. Plx1 recruited to XErp1 phosphorylates it at a site that serves as a phosphodegron for the ubiquitin ligase SCF (Skp, Cullin, F-box) in complex with the F-Box protein βTRCP (beta-transducin repeat containing protein) resulting ultimately in the destruction of XErp1 and hence APC/C^{Cdc20} activation [4]. In contrast, the role of CaN during meiotic exit remains largely elusive. Data from porcine and mouse oocytes suggested that CaN activity is required for timely exit from MII, but the relevant substrates are not known [15,17]. In *Xenopus* oocytes, CaN is also required for proper release from the MII arrest. Yet, the underlying molecular mechanisms remained elusive. One study reported that CaN inhibition interferes with the SCF^{βTRCP}-mediated destruction of XErp1 resulting in impaired APC/C^{Cdc20} activation [14]. Another study came to the conclusion that CaN does not act on XErp1, but that it promotes APC/C activation by removing inhibitory phosphorylations on Cdc20 [13]. However, it remained elusive whether CaN directly or indirectly mediates the dephosphorylation of any of the known three inhibitory phosphorylation sites Thr64, Thr68, and Thr79 (human/mouse: Thr55, Thr59, and Thr70) of Cdc20 [18–21]. In somatic cells, PP2A was shown to activate Cdc20 by dephosphorylating it at these inhibitory sites [19,22].

Here, we aimed to dissect in detail the role of CaN during meiotic exit. For these studies, we employed the well-established cell-free extract system of *Xenopus* oocytes [23,24]. We discover that CaN promotes APC/C^{Cdc20} activation by acting on both the APC/C inhibitor XErp1 and the APC/C co-activator Cdc20. Specifically, we demonstrate that CaN inhibition interfered with timely destruction of XErp1. Using a non-degradable XErp1 version, we could demonstrate that CaN inhibition unexpectedly accelerated the

1 Department of Biology, University of Konstanz, Konstanz, Germany
2 Konstanz Research School Chemical Biology, University of Konstanz, Konstanz, Germany
3 MRC Laboratory of Molecular Biology, Cambridge, UK
*Corresponding author. Tel: +49 7531 88 3707; Fax: +49 7531 88 4036; E-mail: thomas.u.mayer@uni-konstanz.de

dephosphorylation of XErp1 during meiotic exit. We could demonstrate that CaN dephosphorylates XErp1 at a site that is part of a phosphorylation-dependent recruiting motif for PP2-B'56, which protects XErp1 from inactivating and destabilizing phosphorylation events [5,6,10,11]. In the case of Cdc20, CaN inhibition delayed the calcium-induced dephosphorylation. CaN directly dephosphorylates Cdc20 at Thr68, which when phosphorylated impairs Cdc20 from activating the APC/C [20,22]. Thus, the calcium stimulus at fertilization branches into the activation of CaMKII and CaN, which join efforts to activate the APC/C in a highly efficient manner.

Results and Discussion

To investigate the role of calcineurin during exit from meiosis II, we prepared extracts from mature eggs (CSF extracts) of *Xenopus laevis* (Fig 1A) [23,24] and monitored cyclin B2 levels following calcium-induced release from the MII arrest. In control-treated extracts (DMSO for CsA; buffer for His-CnA$^{420–508}$), cyclin B2 levels markedly declined within 8 min after calcium addition (Figs 1B and EV1A). Inhibition of CaN by CsA or the auto-inhibitory domain of the catalytic subunit CnA [14] fused to a His-tag (His-CnA$^{420–508}$) slightly delayed the degradation of cyclin B2 (Fig 1B). Thus, our data confirmed that CaN inhibition results in a mild but reproducible delay in APC/C activation at exit from MII [13,14].

Depletion of XErp1 from CSF extract or addition of constitutively active CaMKII is sufficient to activate the APC/C in the absence of the calcium stimulus, indicating that the CaMKII-mediated destruction of XErp1 constitutes the major APC/C-activating pathway [4,12]. Notably, CaMKII—like CaN—is activated only very transiently during calcium-induced meiotic exit [12,14]. We therefore speculated that CaN constitutes an auxiliary pathway that supports CaMKII to reduce—within the narrow time window when they are active—the APC/C inhibitory activity of XErp1 to levels sufficiently low to allow exit from meiosis. A corollary of this hypothesis is that conditions that hamper CaMKII-mediated XErp1 inactivation should increase the contribution of CaN to meiotic exit. To test this, we first challenged the release from MII by titrating the amount of calcium added to CSF extracts. As expected, upon a strong calcium stimulus ($\geq$ 500 μM) we observed the complete degradation of cyclin B2 within 20 min in DMSO- as well as in CsA-treated extracts (Fig 1C). Importantly, at intermediate calcium concentrations (300 and 400 μM), cyclin B2 degradation was markedly impaired in CaN-inhibited extracts. Lower calcium concentrations (200 μM) failed to sufficiently activate the APC/C, even in the presence of CaN activity. Similar results were obtained when the experiment was repeated using FK506 to inhibit CaN (Fig EV1B). Second, we challenged exit from MII by adding increasing amounts of the CaMKII inhibitory peptide CaMKII$^{281–309}$. While high concentrations (300 μg/ml) completely blocked calcium-induced cyclin B2 degradation irrespective of CaN activity, at intermediate concentrations (100 μg/ml), efficient cyclin B2 degradation occurred only in DMSO- but not CsA-treated extracts (Fig EV1C). Third, we aggravated meiotic exit by adding increasing amounts of ectopic *in vitro*-translated (IVT) Myc-tagged wild-type XErp1 (Myc-XErp1^{wt}) to CSF extracts. Since XErp1 undergoes phosphorylation-dependent mobility shifts in SDS–PAGE, samples were treated with λ-phosphatase before immunoblot analyses. As expected, in the absence of ectopic XErp1 and at high calcium concentrations, CaN inhibition had only a mild effect on cyclin B2 destruction (Fig 1D, lane 1–3 vs. 4–6). However, when the amount of XErp1 in the extract was roughly doubled (1:160 IVT Myc-XErp1^{wt}), cyclin B2 degradation was significantly inhibited in CsA-treated extracts compared to the DMSO control (lane 7–9 vs. 10–12). Further increases in XErp1^{wt} interfered with cyclin B2 degradation in control- as well as in CsA-treated extracts (lanes 13–24). The effect of ectopic XErp1 on cyclin B2 degradation was dependent on XErp1's APC/C inhibitory activity as XErp1 deficient in APC/C inhibition had no effect (Fig EV1D). Notably, we observed that endogenous as well as ectopic XErp1 was less efficiently degraded in CsA-treated extracts (Fig 1D). To confirm this, we repeated the assay with increased temporal resolution. CaN inhibition had no significant effect on the initial degradation of endogenous and exogenous XErp1 (Figs 1E and EV1E). However, while in control extracts the destruction of endogenous and exogenous XErp1 continued, it ceased in CsA-treated extracts. As expected, the decline in XErp1 destruction in CsA-treated extracts coincided with a decreased rate of cyclin B2 degradation (Figs 1E and EV1E). Thus, in line with previous reports [14] these data suggest that CaN contributes to meiotic exit by promoting the destruction of XErp1.

Next, we sought to gain more insight into the mechanism of CaN-mediated XErp1 destruction. At fertilization, the coordinated activities of CaMKII and Plx1 target XErp1 for SCF$^{\beta TRCP}$-mediated degradation [4,10,16]. Based on this, we investigated whether CaN affects the phosphorylation state of XErp1 following fertilization. To uncouple the phosphorylation of XErp1 from its destruction, we supplemented CSF extract with Myc-XErp1 that carried mutations in the SCF$^{\beta TRCP}$ phospho-degrons (DSG^{-} DSA^{-}, Fig 2A) [4,6]. Furthermore, to prevent that stable Myc-XErp1$^{DSG-DSA-}$ interfered with APC/C activation we introduced an additional mutation in its zinc-binding region (ZBR^{-}), which abrogates XErp1′s APC/C inhibitory activity [4,9]. Addition of calcium induced an immediate hyperphosphorylation of Myc-XErp1$^{DSG-DSA-ZBR-}$ that was not affected by inhibition of CaN with CsA (Fig 2B). However, after around 10 min the hyperphosphorylation of ectopic XErp1 was gradually reversed in CsA-treated extracts (see arrow in Fig 2B and in the pseudocolored image in Fig EV2A) and this was less pronounced in control-treated extracts. Importantly, the same effect was observed when CaN was inhibited by FK506 (Fig EV2B). Notably, the effect of CaN inhibition on the dephosphorylation of XErp1$^{DSG-DSA-ZBR-}$ (Fig 2B) temporally correlated with its effect on the destruction of XErp1^{wt} (Fig 1E), suggesting that CaN might control phosphorylation events involved in XErp1 destruction. As expected, under these conditions (600 μM calcium, ectopic XErp1 deficient in APC/C inhibition) CaN inhibition only mildly affected cyclin B2 destruction. From these data, we conclude that CaN activity is required to, counterintuitively, maintain XErp1 in a hyperphosphorylated state during meiotic exit. One explanation for this unexpected finding could be that CaN negatively regulates the activity of another phosphatase acting on XErp1. The only known XErp1 phosphatase is PP2A-B'56, which is recruited to XErp1 by a canonical B′56 binding motif [10,11,25]. Phosphorylation of XErp1 on Ser335, Thr336, and Ser342 by p90^{RSK} significantly increases its affinity for PP2A-B′56 [5,6,10,11,25]. If CaN interferes with the dephosphorylation of XErp1 by PP2A-B'56, preventing the recruitment of PP2A-B'56 to XErp1 should abolish the effect of CaN inhibition. To test this, we mutated all three p90^{RSK} phosphorylation

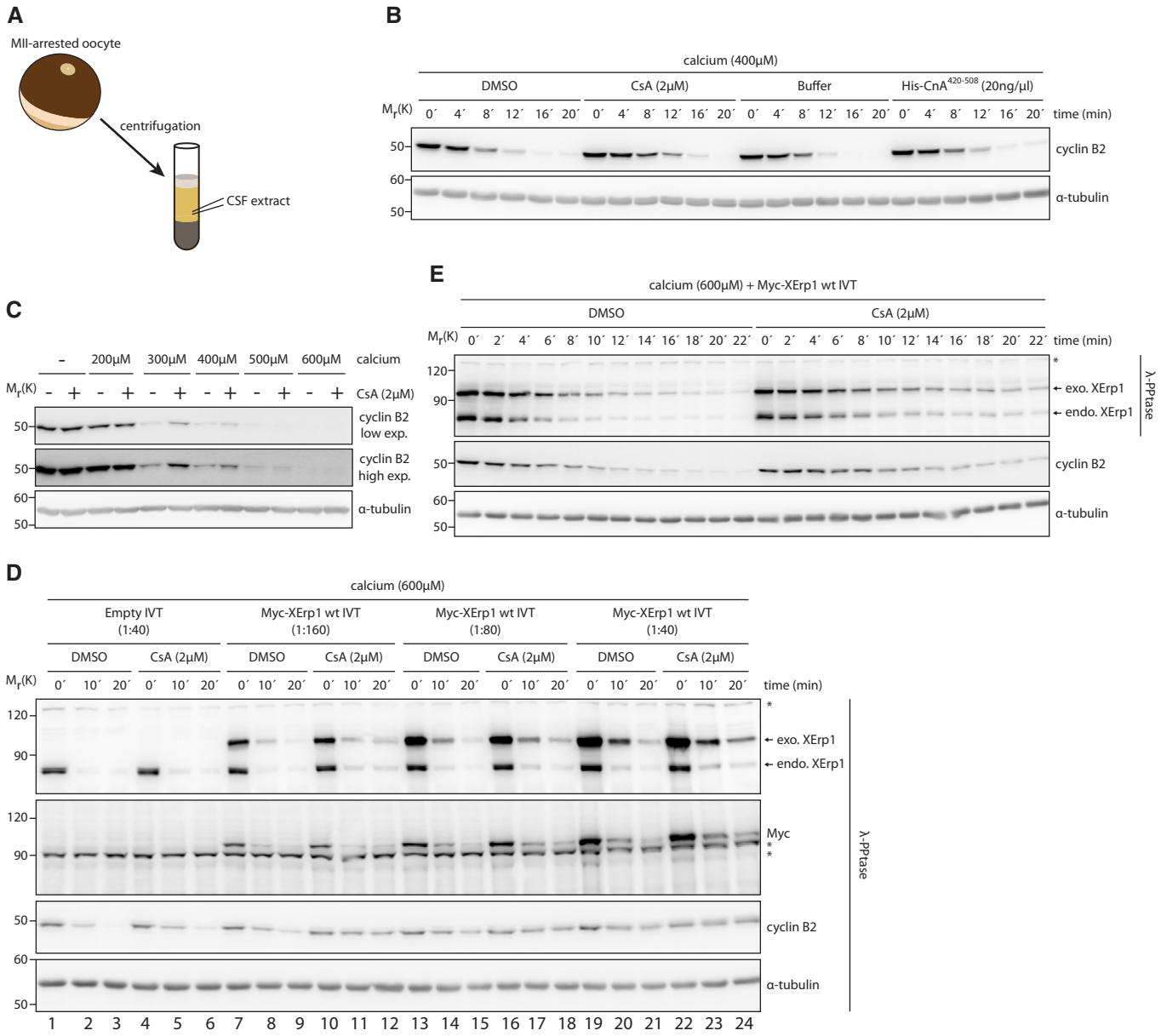

Figure 1. Calcineurin is required for efficient cyclin B2 and XErp1 degradation at meiotic exit.

A Scheme for the preparation of CSF extract.

B CSF extract was treated with DMSO, CsA, buffer or His-CnA$^{420–508}$ at the indicated concentrations. Meiotic exit was induced by calcium addition, and samples were taken at the indicated time points. Samples were immunoblotted for cyclin B2. The cyclin B2 membrane was stripped and reprobed for α-tubulin.

C CSF extract was treated with DMSO or CsA. Both reactions were divided and supplemented with the indicated amounts of calcium or H_2O. After 20 min, samples were taken and immunoblotted for cyclin B2 for which a low and high exposure is shown. The cyclin B2 membrane was stripped and reprobed for α-tubulin.

D CSF extract was supplemented with Myc-XErp1 wt IVT at the indicated dilutions. An empty IVT reaction not expressing Myc-XErp1 served as control. All reactions were divided and treated with DMSO or CsA. Calcium was added to all reactions, and samples were taken at the indicated time points, treated with λ-phosphatase and immunoblotted for XErp1, the Myc-tag, cyclin B2, and α-tubulin. Asterisks indicate unspecific bands.

E CSF extract was supplemented with Myc-XErp1 wt IVT. The reaction was divided and treated with DMSO or CsA. Both reactions were treated with calcium, and samples were taken at the indicated time points and as indicated incubated with λ-phosphatase. Samples were immunoblotted for XErp1 and cyclin B2. The cyclin B2 membrane was stripped and reprobed for α-tubulin. Asterisk indicates unspecific bands.

Source data are available online for this figure.

sites to alanine residues (Myc-XErp1$^{DSG-DSA-ZBR-Rsk3A}$) and analyzed its dephosphorylation upon meiotic exit. As shown before (Fig 2B), Myc-XErp1$^{DSG-DSA-ZBR-}$ was initially hyperphosphorylated after calcium addition and the subsequent dephosphorylation was accelerated by CsA (Fig 2C, lanes 1–6 vs. 7–12). Myc-XErp1$^{DSG-DSA-ZBR-Rsk3A}$ was already hyperphosphorylated

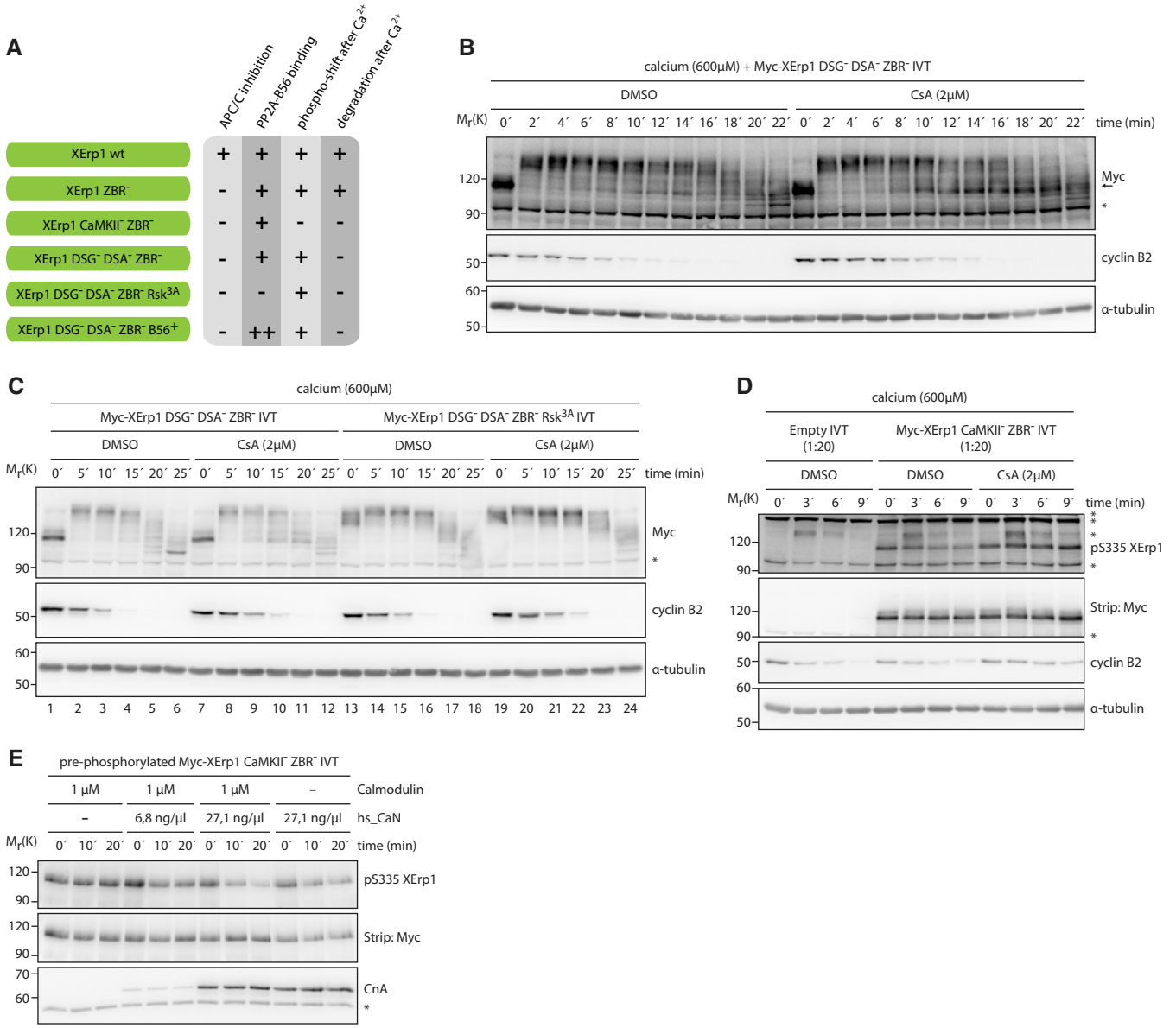

Figure 2. Calcineurin affects the phospho-regulation of XErp1.

A Schematic representation of the XErp1 variants and their characteristics used in this study.

B CSF extract was supplemented with Myc-XErp1 DSG^{-} DSA^{-} ZBR^{-} (S33N S38N S284N S288N C583A) IVT and as indicated treated with DMSO or CsA. Both reactions were treated with calcium and samples were taken at the indicated time points. Samples were immunoblotted for the Myc-tag, cyclin B2, and α-tubulin. A pseudocolored representation of the Myc immunoblot is shown in Fig EV2A. Arrow marks the meiotic phosphorylation state of Myc-XErp1. Asterisk indicates unspecific bands.

C CSF extract was supplemented with Myc-XErp1 DSG^{-} DSA^{-} ZBR^{-} (S33N S38N S284N S288N C583A) IVT that was either wild-type or mutated to alanine at the p90^{RSK}-target sites S335, T336, and S342 (Rsk^{3A}). Both reactions were divided and treated with DMSO or CsA. Calcium was added, and samples were taken at the indicated time points. Samples were immunoblotted for the Myc-tag and cyclin B2. The cyclin B2 membrane was stripped and reprobed for α-tubulin. Asterisk indicates unspecific bands.

D CSF extract was treated with Myc-XErp1 CaMKII^{-} ZBR^{-} (T195A C583A) IVT. An empty IVT reaction not expressing XErp1 was used as control. The extracts were treated with DMSO or CsA as indicated. Calcium was added, and samples were taken at the indicated time points and immunoblotted for cyclin B2, pSer335 XErp1, and α-tubulin. The pSer335 XErp1 membrane was stripped and reprobed for the Myc-tag. Asterisks indicate unspecific bands.

E Myc-XErp1 CaMKII^{-} ZBR^{-} (T195A C583A) IVT was *in vitro* phosphorylated by recombinant PKA and isolated by α-Myc immunoprecipitation. The immunoprecipitate was supplemented with calcium and treated with recombinant hs_CaN and calmodulin as indicated. Samples were taken at the indicated time points and immunoblotted for the catalytic calcineurin subunit CnA and pSer335 XErp1. The pSer335 XErp1 membrane was stripped and reprobed for the Myc-tag. Asterisk indicates the IgG heavy chain.

Source data are available online for this figure.

in CSF extract (lane 1/7 vs. 13/19), suggesting in line with previous reports [10,11] that PP2A-B'56 antagonizes phosphorylation of XErp1 by Cdk1 and other kinases during the MII arrest. Importantly, the dephosphorylation of Myc-XErp1$^{DSG-DSA-ZBR-Rsk3A}$ following calcium treatment was not significantly different in control-treated extracts compared to the CsA samples (lanes 13–18 vs. 19–24) supporting our hypothesis that CaN negatively affects the PP2A-B'56-mediated dephosphorylation of XErp1. To further corroborate this hypothesis, we performed the reverse experiment in that we mutagenized the p90^{RSK}-dependent PP2A-B'56 binding site in XErp1 [25] to a phosphorylation-independent binding motif (LSTLRERGSQS^{344} → LPTIREEEEQS^{344}, XErp1^{B56+}). Co-IP experiments confirmed that these mutations resulted in stronger PP2A-B'56 binding (Fig EV2C). Importantly, the phosphorylation state of Myc-XErp1$^{DSG-DSA-ZBR-B56+}$ upon calcium stimulation was not affected by CaN inhibition, suggesting that the regulation of XErp1 by CaN was bypassed under these conditions (Fig EV2D). The most direct explanation for this would be that CaN dephosphorylates the p90^{RSK}-target sites. To test this, we raised a phosphorylation-specific antibody against Ser335 (pSer335). Due to low sensitivity of the antibody, we had to supplement extracts with IVT XErp1. To prevent the calcium-induced upshift, which would hamper the analyses of pSer335, we used XErp1 with a mutation in the CaMKII phosphorylation site (Fig EV3A, Thr195→A, CaMKII^{-}). Adding Myc-XErp1$^{CaMKII-ZBR-}$ to CSF extract resulted in a pSer335 signal whose strength correlated with the amount of added protein (Fig EV3B). This signal was specific for pSer335 because it was lost upon λ-phosphatase treatment or mutation of Ser335 to alanine (Fig EV3C). After having validated the antibody, we analyzed the phosphorylation state of Ser335 during meiotic exit. Indeed, the pSer335 signal decreased upon calcium-induced MII release (Fig 2D). The pSer335 signal did not disappear completely in the DMSO control probably because the amount of added IVT XErp1 exceeded the capacity of the phosphatases acting on XErp1. Importantly, in CsA-treated extract the pSer335 signal did not significantly decline upon calcium stimulation, indicating that CaN directly or indirectly mediates the dephosphorylation of Ser335 during meiotic exit. To test whether CaN directly dephosphorylates pSer335, we established an *in vitro* phosphatase assay. Specifically, Myc-XErp1$^{CaMKII-ZBR-}$ was incubated with recombinant protein kinase A (PKA), which phosphorylates XErp1 at Ser335 during early embryonic divisions [26]. Pre-phosphorylated XErp1 was subsequently incubated with recombinant human CaN (hs_CaN), which shows high sequence conservation with *Xenopus* CaN, in the presence of calcium with or without calmodulin [27,28]. In the absence of CaN, the pSer335 signal remained constant throughout the time course (Fig 2E). In the presence of calmodulin, incubation of pre-phosphorylated XErp1 with hs_CaN resulted in a dose-dependent decrease in the pSer335 signal. In the absence of calmodulin, pSer335 was weakly dephosphorylated by CaN confirming previous reports [29] that CaN even in the absence of its co-activator has some basal activity. Studies on mammalian Emi2 have suggested that phosphorylation of Ser385 (Ser335 in XErp1) increases the affinity for B′56 roughly 2,6-fold [25]. We therefore speculated that CaN contributes to the inactivation and destabilization of XErp1 due to a weakened association of the protective phosphatase PP2A-B′56 [10,11]. To test this, we analyzed whether CaN inhibition affects the association of XErp1 with PP2A-B'56 during meiotic exit. Unfortunately, co-IP experiments using ectopic XErp1 and PP2A-B'56 did not yield conclusive results. Irrespective of this, these experiments indicate that CaN contributes to XErp1 destabilization at fertilization by dephosphorylating it directly at Ser335.

Next, we analyzed the function of CaN in the dephosphorylation of Cdc20 at meiotic exit. During CSF arrest, Cdc20 is phosphorylated by Cdk1 at three threonine residues (Thr64, Thr68, and Thr79) and these phosphorylation events prevent Cdc20 from activating the APC/C [18,20,22]. In contrast, the APC/C has to be phosphorylated by Cdk1 on multiple serine residues to be active [30–32]. The paradox of how such a regulation allows the formation of active APC/C^{Cdc20} was recently solved by demonstrating that PP2A-B55, the phosphatase acting on Cdc20 and APC/C in mitosis, has a strong preference for pThr resulting in temporally ordered dephosphorylation events with Cdc20 being dephosphorylated before the APC/C [19]. To test whether the same mechanism applies in meiosis, we analyzed the dephosphorylation kinetics of ectopic wild-type and mutant Cdc20 with the three inhibitory threonine sites mutated to serine (3T→S) during meiotic exit. Using Phos-tag™ SDS–PAGE [33], which enhances the mobility shift of phosphorylated proteins, we observed that Flag-Cdc20^{wt} was quickly dephosphorylated with the first signs of dephosphorylation being detectable at 5 min after calcium addition (Fig 3A). Faster migrating forms of the APC/C subunit Cdc27 were not detectable until 20 min in line with the idea that differential dephosphorylation kinetics allow the formation of active APC/C^{Cdc20} [19]. Importantly, the 3T→S mutation abolished the time lag between Cdc20 and APC/C dephosphorylation. Please note that this did not affect cyclin B2 destruction due to the presence of endogenous Cdc20. From these data, we conclude that a calcium-activated phosphatase with a pThr preference acts on Cdc20. Given the reported preference of CaN for pThr and the effect of its inhibition on APC/C^{Cdc20} activation [13,34], we analyzed next in detail the effect of CaN inhibition on the phosphorylation state of Cdc20. In Phos-tag™ SDS–PAGE, endogenous Cdc20 showed a strong phosphorylation-dependent mobility shift in CSF extract, which was quickly reverted upon calcium addition (Fig 3B). We observed also late dephosphorylation events (16–24 min) occurring after the reported activity window of CaN [13,14]. Non-Phos-tag™ SDS–PAGE confirmed that Cdc20 levels remained constant during the experiment. Importantly, CaN inhibition by CsA or FK506 strongly inhibited the early but not late dephosphorylation of Cdc20 (Figs 3B and EV4A and B). Thus, in line with previous reports [13], we conclude from these data that CaN—directly or indirectly—mediates the initial dephosphorylation of Cdc20, while other phosphatase(s) act later on it. Next, we analyzed whether CaN targets the inhibitory sites of Cdc20. Given that all three inhibitory sites seem to be equally important for Cdc20 regulation [20], we focused on Thr68 for which suitable phospho-specific antibodies were available. After immunoprecipitating IVT Flag-Cdc20 from CSF extract, the pThr68 antibody detected a signal that was absent when the samples were treated with λ-phosphatase or when Thr68 was mutated to alanine (Fig EV4C) indicating that Cdc20 is phosphorylated at Thr68 in MII. Adding calcium resulted in a fast dephosphorylation of Thr68, and importantly, this was strongly impaired in CsA-treated extracts (Fig 3C). Next, we analyzed whether CaN directly dephosphorylates Thr68. Specifically, we incubated Flag-Cdc20 in CSF extract, re-isolated it, and incubated pre-phosphorylated Flag-Cdc20 with recombinant

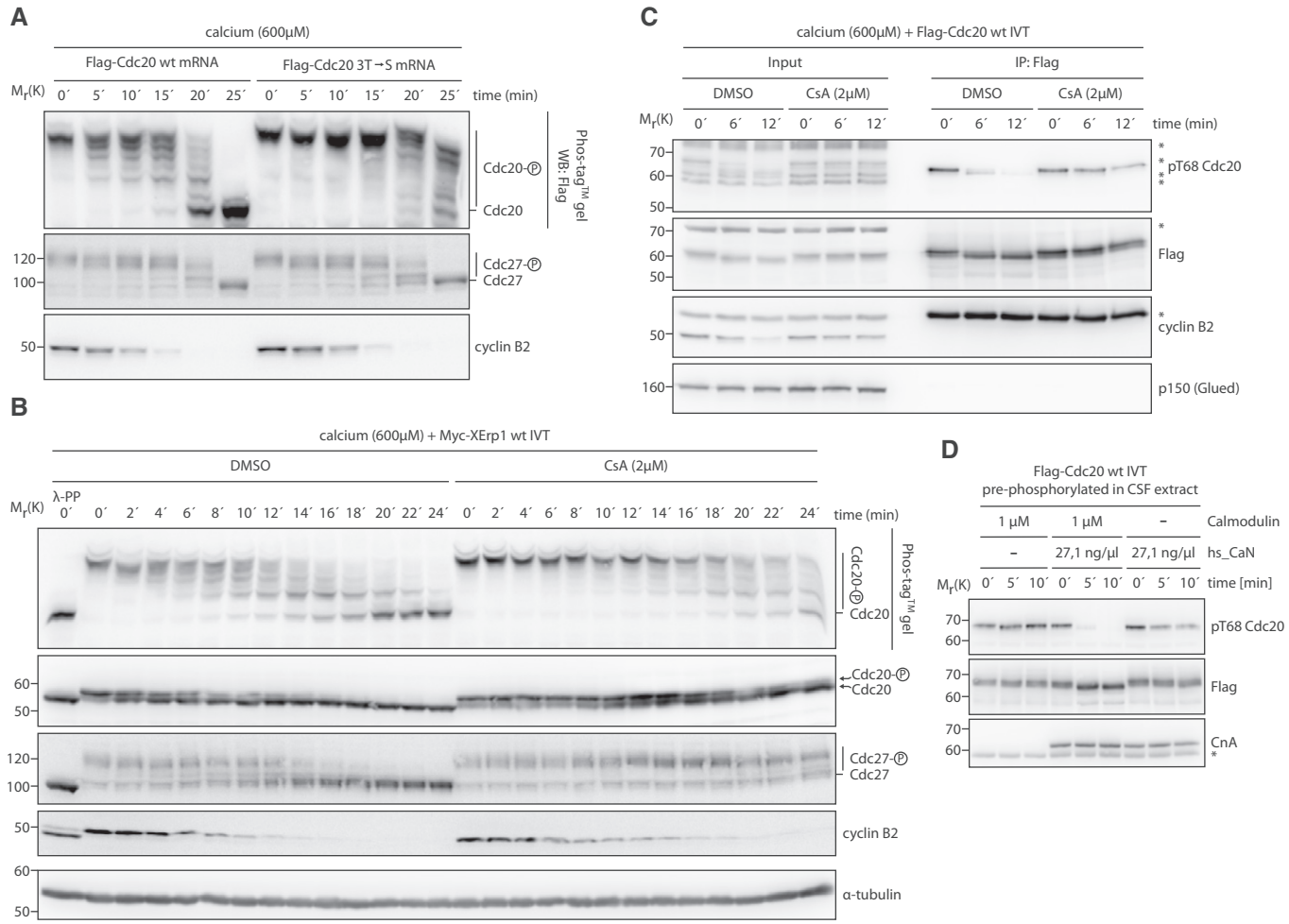

Figure 3. Thr68 of Cdc20 is a target site of calcineurin.

A CSF extract was supplemented with mRNA encoding Flag-Cdc20 that was either wild-type or mutated to serine at Thr64, Thr68, and Thr79 (3T→S). After expression, calcium was added, samples were taken at the indicated time points and resolved by either conventional or Phos-tag™ SDS–PAGE. Samples were immunoblotted for the Flag-tag, Cdc27, and cyclin B2.

B CSF extract was supplemented with Myc-XErp1 wt IVT and treated with DMSO or CsA. Calcium was added, samples were taken at the indicated time points, resolved by either conventional or Phos-tag™ SDS–PAGE and immunoblotted for Cdc20, Cdc27, and cyclin B2. A control sample was treated with λ-phosphatase. A pseudocolored representation of the Cdc20 and the Cdc27 immunoblots is shown in Fig EV4A. The cyclin B2 membrane was stripped and reprobed for α-tubulin.

C CSF extract was supplemented with Flag-Cdc20 wt IVT coupled to α-Flag beads. Calcium was added, and Flag-Cdc20 was isolated by α-Flag immunoprecipitation at the indicated time points. Input and pellet (IP: Flag) samples were immunoblotted for the Flag-tag, pThr68 Cdc20 and p150(Glued). The pThr68 Cdc20 membrane was stripped and reprobed for cyclin B2. Asterisk in the cyclin B2 immunoblot indicates the IgG heavy chain. Asterisks in other immunoblots indicate unspecific bands.

D CSF extract was supplemented with Flag-Cdc20 wt IVT. Flag-Cdc20 was re-isolated by α-Flag immunoprecipitation, supplemented with calcium and treated with recombinant hs_CaN and calmodulin as indicated. Samples were taken at the indicated time points and immunoblotted for the Flag-tag and pThr68 Cdc20. The pThr68 Cdc20 membrane was stripped and reprobed for the catalytic calcineurin subunit CnA. Asterisk indicates the IgG heavy chain.

Source data are available online for this figure.

hs_CaN. As in the case of Ser335 of XErp1, we observed that Thr68 of Cdc20 was efficiently dephosphorylated by CaN in the presence of its co-activator calmodulin, but not in its absence (Fig 3D). From these data, we conclude that Cdc20 is phosphorylated at Thr68 during metaphase II and that CaN directly dephosphorylates Cdc20 at this inhibitory site during meiotic exit.

In summary, based on our comprehensive analyses we propose the following model of CaN function during exit from meiosis (Fig 4A). During the MII arrest of *Xenopus* oocytes, the activity of the APC/C is kept low by the presence of its inhibitor XErp1 and by inhibitory phosphorylation of its co-activator Cdc20 [4,18,20]. Fertilization triggers a transient calcium wave in the oocyte, and this signal branches in the activation of CaMKII and CaN [12–14,35]. CaMKII acts as a priming kinase for Plx1, which in turn creates a phosphorylation-dependent recognition motif (DpSGxxxpS[38]) in XErp1 for the E3 ligase $SCF^{\beta TRCP}$ [4,16]. In parallel, CaN dephosphorylates XErp1 at Ser335 and this dephosphorylation event impedes PP2A-B'56 from protecting XErp1 against inhibitory phosphorylations (Fig 2). Thus, CaN supports CaMKII in targeting XErp1 for destruction and the concerted effort of both enzymes ensures that

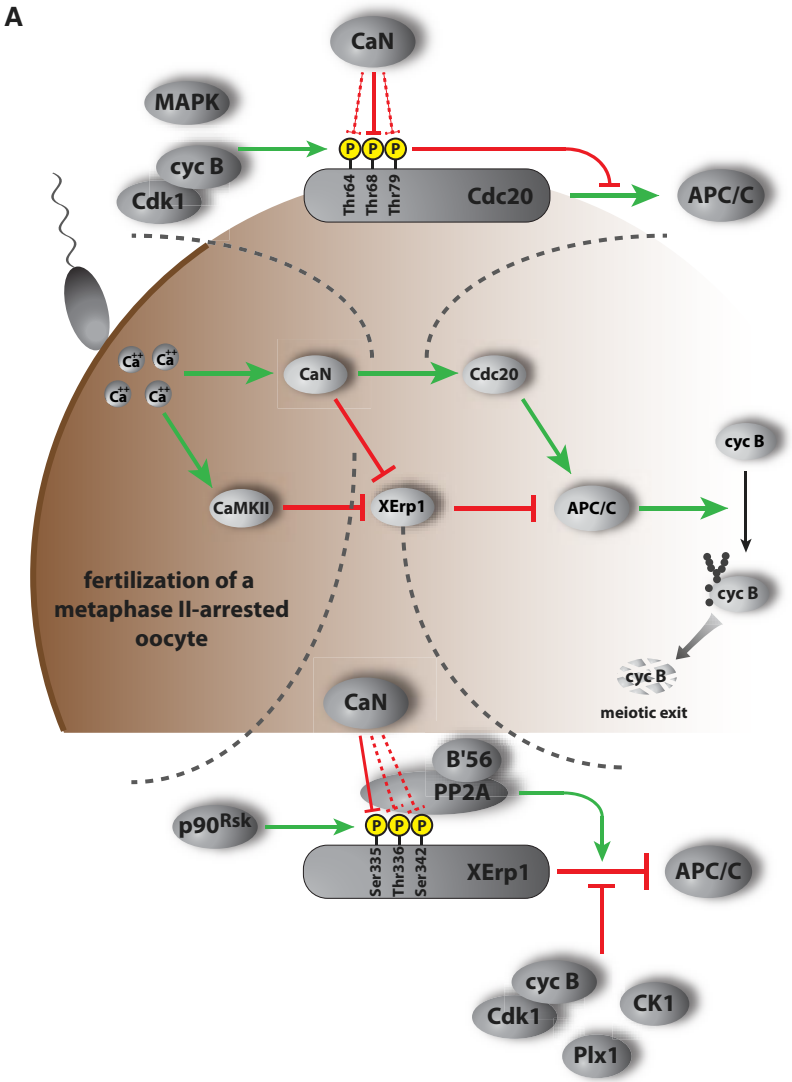

Figure 4. Working model.

A Working model depicting the function of CaMKII and CaN in APC/C activation at meiotic exit in *Xenopus laevis* oocytes. Green and red connections indicate activating and inhibitory, respectively, relationships.

XErp1 levels drop fast enough within the narrow time window of CaMKII and CaN activity. In parallel, CaN contributes to APC/C activation by dephosphorylating its co-activator Cdc20 at the inhibitory site Thr68 (and possibly also at Thr64 and Thr79, Fig 3). Active APC/C^{Cdc20} liberated from its inhibitor XErp1 subsequently targets cyclin B and securin for degradation resulting in sister chromatid segregation and meiotic exit. So far, we could not identify known binding motifs of CaN on XErp1 and Cdc20, e.g., "PxIxIT" or "LxVP" motifs [36–38]. Thus, future studies will be important to decipher the exact binding mode of CaN to Cdc20 and XErp1. Reportedly, CaN activates at meiotic exit the translation regulator maskin, which then suppresses cyclin B translation [39]. This reduction in cyclin B synthesis might synergize with increased APC/C activation to ensure low cyclin B levels at the transition to interphase of the first embryonic division.

Materials and Methods

CSF extracts

Xenopus laevis frogs were bred and maintained under laboratory conditions at the animal research facility, University of Konstanz, and all procedures performed were approved by the Regional Commission, Freiburg, Germany. Female *Xenopus laevis* frogs were primed 3-7 days before extract preparation by subcutaneous injection of 50 units PMSG (Intervet). On the evening before extract preparation, the frogs were subcutaneously injected with 800 units hCG (Intervet) to induce ovulation. The frogs were kept in 1× MMR buffer (5 mM HEPES; 0.1 mM EDTA; 100 mM NaCl; 2 mM KCl; 1 mM $MgCl_2$; 2 mM $CaCl_2$; pH = 7.8) at 19°C overnight. On the following morning, the mature eggs were collected and washed in 1xMMR if necessary.

The oocytes were dejellied by incubation in Dejellying Solution (2% (w/v) cysteine; 100 mM KCl; 1 mM $MgCl_2$; 0.1 mM $CaCl_2$; pH = 7.8) until they visibly compacted. The oocytes were washed 4× with 1× CSF-XB (10 mM HEPES; 100 mM KCl; 2 mM $MgCl_2$; 0.1 mM $CaCl_2$; 50 mM Sucrose; 5 mM EGTA; pH = 7.7). The oocytes were transferred to centrifugation tubes containing 750 µl 1× CSF-XB supplemented with 100 µg/ml cytochalasin B (Cayman Chemical). The oocytes were compacted for 1 min with 164 g at 4°C and for 1 min with 656 g at 4°C. Excess supernatant was removed, and the oocytes were crushed by centrifugation for 10 min with 16,398 *g* at 4°C. The CSF extract was retrieved with a syringe and supplemented with 10 µg/ml cytochalasin B (Cayman Chemical). The extract was kept on ice until used in experiments.

Unless otherwise stated, all experiments were performed at 20°C. CaN inhibitors were added for 5 min before meiotic exit was induced. Cyclosporin A (Calbiochem) and FK-506 (Sigma-Aldrich) were dissolved in DMSO and added at a final concentration of 2 µM and 3 µM, respectively. His-$CnA^{420–508}$ was dissolved in dialysis buffer and added at 20 ng/µl. CaM Kinase II Inhibitor 281–309 ($CaMKII^{281–309}$, Calbiochem) was dissolved in 1× CSF-XB and added at the indicated concentrations. All *in vitro* transcription and translation reactions (IVTs) were incubated in CSF extract for at least 20 min prior further treatments. IVTs without a protein-coding plasmid (empty) were used as control.

Recombinant proteins and mRNAs

His-$CnA^{420–508}$ (*Xenopus laevis*, 6xHis-tag, aa420–508) was expressed in BL21(RIL) bacteria, purified by Ni^{2+}-NTA agarose affinity chromatography and dialyzed against dialysis buffer (20 mM HEPES; 150 mM KCl; 1 mM DTT; 10% (v/v) glycerol; pH = 7.7). Calmodulin was purchased from Sigma-Aldrich. Recombinant human calcineurin dimer (hs_CaN) was purchased from R&D systems. Recombinant PKA was purchased from Calbiochem. All other proteins were expressed as IVTs in TNT® SP6 High-Yield Wheat Germ Protein Expression System (Promega) according to the manufacturer's instructions: Myc-XErp1 wt (*Xenopus laevis*, 6xMyc-tag, wild-type); Myc-XErp1 ZBR^- (*Xenopus laevis*, 6xMyc-tag, C583A); Myc-XErp1 DSG^- DSA^- ZBR^- (*Xenopus laevis*, 6xMyc-tag, S33N S38N S284N S288N C583A); Myc-XErp1 DSG^- DSA^- ZBR^- Rsk^{3A} (*Xenopus laevis*, 6xMyc-tag, S33N S38N S284N S288N S335A T336A S342A C583A); Myc-XErp1 DSG^- DSA^- ZBR^- $B56^+$ (*Xenopus laevis*, 6xMyc-tag, S33N S38N S284N S288N S335P L337I R340E G341E S342E C583A); Myc-XErp1 $CaMKII^-$ ZBR^- (*Xenopus laevis*, 6xMyc-tag, T195A C583A); Myc-XErp1 $CaMKII^-$ ZBR^- S335A (*Xenopus laevis*, 6xMyc-tag, T195A S335A C583A); Flag-Cdc20 wt (*Xenopus laevis*, 3xFlag-tag, wild-type); Flag-Cdc20 T68A (*Xenopus laevis*, 3xFlag-tag, T68A); Flag-Cdc20 3T→S (*Xenopus laevis*, 3xFlag-tag, T64S T68S T79S). mRNA for Flag-B′56ε (*Xenopus laevis*, 3x-Flag-tag, wild-type) was prepared using the mMESSAGE mMACHINE™ T7 Ultra Transcription Kit (Invitrogen) according to the manufacturer's instructions. Further details will be provided upon request.

Immunoblots

Where indicated, 15 µM Phos-tag™ (Wako Pure Chemical Industries) and 30 µM $MnCl_2$ were added to standard SDS-PA gels. Proteins were transferred to nitrocellulose membranes (Whatman Protran). Membranes were blocked in 5%(w/v) milk/PBST for 30 min. Membranes that were probed with phospho-antibodies were blocked with 5%(w/v) BSA/TBST. Primary antibodies were diluted in 5%(w/v) milk/PBST and primary phospho-antibodies in 5%(w/v) BSA/TBST. All primary antibodies were added to the membranes at 4°C overnight. Membranes were washed three times with PBST or TBST for 10 min. Secondary antibodies (HRP-coupled, α-mouse and α-rabbit, Dianova) were diluted 1:5,000 in the solution used for blocking and incubated at room temperature for 1 h. Membranes were washed again three times with PBST or TBST for 10 min. The membranes were covered with ECL solution (TrisCl pH 8.5; 0,012% H_2O_2; 225 µM P-coumaric acid (Sigma-Aldrich); 1.25 mM luminol (Fluka)). Chemiluminescent signals were detected with a LAS-3000 (GE Healthcare Life Sciences).

Immunoblot analysis

Band intensities in immunoblots were quantified using ImageJ. Calculations were done using Microsoft Excel 2013. Bar graphs were generated using GraphPad Prism 6. Pseudocolor representations of immunoblots were made using Fujifilm Multi Gauge V3.0.

Antibodies

XErp1 (diluted 1:1,000) and Cdc27 (1:500) antibodies were described before [26]. Cyclin B2 antibody (1:500) was purchased from Santa Cruz (sc-53239). Calcineurin A antibody (1:500) was purchased from BD Transduction Laboratories (No. 610260). Cdc20 antibody (1:500) was purchased from Abcam (ab18217). p150 (Glued) antibody (1:1,000) was purchased from BD Transduction Laboratories (No. 610473). Flag-tag antibodies (for immunoprecipitation and immunoblot) were diluted 1:1,000 and purchased from Sigma-Aldrich (F1804) or generated by immunization of rabbits with Flag-peptide (NH2-CMDYKDHDGDYKDHDIDYKDDDDK-COOH) and purification against the Flag-peptide. Phospho-Ser335 XErp1 antibody (1:1,000) was generated by immunization of rabbits with pS335 peptide (NH2-CRRLpSTLRER-COOH) and positive purification against the pS335 peptide followed by negative purification against S335 peptide (NH2-CRRLSTLRER-COOH). Myc-tag antibody for immunoprecipitation and immunoblot (1:100) was purified from hybridoma cells (9E10). α-Tubulin antibody (1:100) was purified from hybridoma cells (DSHB 12G10). Phospho-Thr68 Cdc20 antibody was a gift from J. Nilsson.

λ-phosphatase treatment

Extract samples were dephosphorylated by dilution in five volumes of λ-phosphatase Mix (137 mM NaCl; 2.7 mM KCl; 10 mM Na_2HPO_4; 2 mM KH_2PO_4; 1 mM $MnCl_2$; 1× Protease Inhibitor Complete (Roche); 0.2 µg/µl 6xHis-SUMO-λ-PPtase; pH = 7.4) and incubation for 45 min at 23°C. Bead samples were resuspended in λ-phosphatase Mix and incubated for 45 min at 23°C.

Analysis of phospho-Thr68 Cdc20

15.2 µl CSF extract was supplemented with 0.8 µl Flag-Cdc20 IVT. The mixture was added to 1 µg α-Flag antibodies coupled to

Dynabeads® Protein G (Thermo Fisher). The reaction was incubated for 60 min. 50 µl Wash Buffer (20 mM HEPES; 100 mM KCl; 5 mM $MgCl_2$; 0.025% Tween-20; 5 mM β-glycerophosphate; 2 mM NaF; pH = 7.5) was added, and the whole supernatant was removed. The beads were washed three times with Wash Buffer. The beads were directly resuspended in 30 µl 1.5× Laemmli Sample Buffer or treated with λ-phosphatase.

In vitro phosphatase assays

XErp1: 2 µl Myc-XErp1 IVT were diluted in 8 µl CSF-XB Buffer (10 mM HEPES; 100 mM KCl; 2 mM $MgCl_2$; 0.1 mM $CaCl_2$; 50 mM sucrose; 5 mM EGTA; pH = 7.7) and added to 0.5 µg α-Myc antibodies coupled to Dynabeads® Protein G (Thermo Fisher). After 1 h incubation at 23°C, the beads were washed four times in Kinase Buffer (5 mM MOPS; 2.5 mM β-glycerophosphate; 5 mM $MgCl_2$; 1 mM EGTA; 0.4 mM EDTA; 0.05 mM DTT; 0.025% Tween-20; pH = 7.2). The beads were resuspended in 40 µl Kinase Buffer containing 2.5 mM ATP and 1,000 units recombinant PKA (Calbiochem #539481). The reaction was incubated for 30 min at 30°C. The beads were washed seven times in Kinase Buffer and three times in Phosphatase Buffer (50 mM HEPES; 10 mM $CaCl_2$; 5 mM $MgCl_2$; 1 mM DTT; 0.025% Tween-20; 8.8 mM ascorbate; pH = 7.5).

Cdc20: 50.6 µl CSF extract was supplemented with 2.6 µl Flag-Cdc20 IVT. The mixture was added to 3.3 µg α-Flag antibodies coupled to Dynabeads® Protein G (Thermo Fisher). The reaction was incubated for 60 min at 20°C. The beads were washed three times with Phosphatase Buffer supplemented with 5 mM β-glycerophosphate and 2 mM NaF and two times with Phosphatase Buffer.

For both assays, the beads were resuspended in 22 µl Phosphatase Buffer supplemented with hs_CaN (R&D Systems) and calmodulin (Sigma-Aldrich) as indicated. The reaction was incubated at 30°C, and samples were taken at the indicated time points.

Analysis of XErp1 and PP2A-B′56 interaction

80 µl CSF extract was supplemented with 1.9 µg Flag-B′56ε mRNA and 4 µl Myc-XErp1 IVT. The whole reaction was added to 5 µg α-Flag antibodies coupled to Dynabeads® Protein G (Thermo Fisher). The reaction was incubated for 2 h at 23°C. 200 µl Wash Buffer (20 mM HEPES; 100 mM KCl; 5 mM $MgCl_2$; 0.025% Tween-20; 1× Protease Inhibitor Complete (Roche); pH = 7.5) was added, and the whole supernatant was removed. The beads were washed three times with Wash Buffer. The beads were treated with λ-phosphatase.

Statistical analysis

Statistical analysis was carried out using Microsoft Excel. Values are given as mean ± SD. Statistical significance was probed using unpaired two-sided *t*-test (with unequal variance).

Expanded View for this article is available online.

Acknowledgements

We thank S. Mochida and J. Nilsson for reagents. This work was financially supported by the CRC 969 of the German Research Foundation (DFG) and the Konstanz Research School Chemical Biology (KoRS-CB).

Author contributions

AH and TUM designed research; AH and TT performed research; AH and TUM analyzed data; AH and TUM wrote the paper; and AH, TT, and TUM commented on the manuscript.

Conflict of interest

The authors declare that they have no conflict of interest.

References

1. Gerhart J, Wu M, Kirschner M (1984) Cell cycle dynamics of an M-phase-specific cytoplasmic factor in Xenopus laevis oocytes and eggs. *J Cell Biol* 98: 1247 – 1255
2. Gross SD, Schwab MS, Taieb FE, Lewellyn AL, Qian YW, Maller JL (2000) The critical role of the MAP kinase pathway in meiosis II in Xenopus oocytes is mediated by p90(Rsk). *Curr Biol* 10: 430 – 438
3. Masui Y, Markert CL (1971) Cytoplasmic control of nuclear behavior during meiotic maturation of frog oocytes. *J Exp Zool* 177: 129 – 145
4. Schmidt A, Duncan PI, Rauh NR, Sauer G, Fry AM, Nigg EA, Mayer TU (2005) Xenopus polo-like kinase Plx1 regulates XErp1, a novel inhibitor of APC/C activity. *Genes Dev* 19: 502 – 513
5. Inoue D, Ohe M, Kanemori Y, Nobui T, Sagata N (2007) A direct link of the Mos-MAPK pathway to Erp1/Emi2 in meiotic arrest of Xenopus laevis eggs. *Nature* 446: 1100 – 1104
6. Nishiyama T, Ohsumi K, Kishimoto T (2007) Phosphorylation of Erp1 by p90rsk is required for cytostatic factor arrest in Xenopus laevis eggs. *Nature* 446: 1096 – 1099
7. Ohe M, Kawamura Y, Ueno H, Inoue D, Kanemori Y, Senoo C, Isoda M, Nakajo N, Sagata N (2010) Emi2 inhibition of the anaphase-promoting complex/cyclosome absolutely requires Emi2 binding via the C-terminal RL tail. *Mol Biol Cell* 21: 905 – 913
8. Sako K, Suzuki K, Isoda M, Yoshikai S, Senoo C, Nakajo N, Ohe M, Sagata N (2014) Emi2 mediates meiotic MII arrest by competitively inhibiting the binding of Ube2S to the APC/C. *Nat Commun* 5: 3667
9. Tang W, Wu JQ, Chen C, Yang CS, Guo JY, Freel CD, Kornbluth S (2010) Emi2-mediated inhibition of E2-substrate ubiquitin transfer by the anaphase-promoting complex/cyclosome through a D-box-independent mechanism. *Mol Biol Cell* 21: 2589 – 2597
10. Isoda M, Sako K, Suzuki K, Nishino K, Nakajo N, Ohe M, Ezaki T, Kanemori Y, Inoue D, Ueno H, *et al* (2011) Dynamic regulation of Emi2 by Emi2-bound Cdk1/Plk1/CK1 and PP2A-B56 in meiotic arrest of Xenopus eggs. *Dev Cell* 21: 506 – 519
11. Wu JQ, Hansen DV, Guo Y, Wang MZ, Tang W, Freel CD, Tung JJ, Jackson PK, Kornbluth S (2007) Control of Emi2 activity and stability through Mos-mediated recruitment of PP2A. *Proc Natl Acad Sci USA* 104: 16564 – 16569
12. Lorca T, Cruzalegui FH, Fesquet D, Cavadore JC, Mery J, Means A, Doree M (1993) Calmodulin-dependent protein kinase II mediates inactivation of MPF and CSF upon fertilization of Xenopus eggs. *Nature* 366: 270 – 273
13. Mochida S, Hunt T (2007) Calcineurin is required to release Xenopus egg extracts from meiotic M phase. *Nature* 449: 336 – 340
14. Nishiyama T, Yoshizaki N, Kishimoto T, Ohsumi K (2007) Transient activation of calcineurin is essential to initiate embryonic development in Xenopus laevis. *Nature* 449: 341 – 345
15. Suzuki T, Suzuki E, Yoshida N, Kubo A, Li H, Okuda E, Amanai M, Perry AC (2010) Mouse Emi2 as a distinctive regulatory hub in second meiotic metaphase. *Development* 137: 3281 – 3291

16. Rauh NR, Schmidt A, Bormann J, Nigg EA, Mayer TU (2005) Calcium triggers exit from meiosis II by targeting the APC/C inhibitor XErp1 for degradation. *Nature* 437: 1048 – 1052
17. Tumova L, Chmelikova E, Zalmanova T, Kucerova-Chrpova V, Romar R, Dvorakova M, Hoskova K, Petr J (2016) Calcineurin role in porcine oocyte activation. *Animal* 10: 1998 – 2007
18. Chung E, Chen RH (2003) Phosphorylation of Cdc20 is required for its inhibition by the spindle checkpoint. *Nat Cell Biol* 5: 748 – 753
19. Hein JB, Hertz EPT, Garvanska DH, Kruse T, Nilsson J (2017) Distinct kinetics of serine and threonine dephosphorylation are essential for mitosis. *Nat Cell Biol* 19: 1433 – 1440
20. Labit H, Fujimitsu K, Bayin NS, Takaki T, Gannon J, Yamano H (2012) Dephosphorylation of Cdc20 is required for its C-box-dependent activation of the APC/C. *EMBO J* 31: 3351 – 3362
21. Yudkovsky Y, Shteinberg M, Listovsky T, Brandeis M, Hershko A (2000) Phosphorylation of Cdc20/fizzy negatively regulates the mammalian cyclosome/APC in the mitotic checkpoint. *Biochem Biophys Res Commun* 271: 299 – 304
22. Hein JB, Nilsson J (2016) Interphase APC/C-Cdc20 inhibition by cyclin A2-Cdk2 ensures efficient mitotic entry. *Nat Commun* 7: 10975
23. Lohka MJ, Maller JL (1985) Induction of nuclear envelope breakdown, chromosome condensation, and spindle formation in cell-free extracts. *J Cell Biol* 101: 518 – 523
24. Murray AW, Solomon MJ, Kirschner MW (1989) The role of cyclin synthesis and degradation in the control of maturation promoting factor activity. *Nature* 339: 280 – 286
25. Hertz EPT, Kruse T, Davey NE, Lopez-Mendez B, Sigurethsson JO, Montoya G, Olsen JV, Nilsson J (2016) A Conserved Motif Provides Binding Specificity to the PP2A-B56 Phosphatase. *Mol Cell* 63: 686 – 695
26. Tischer T, Hormanseder E, Mayer TU (2012) The APC/C inhibitor XErp1/Emi2 is essential for Xenopus early embryonic divisions. *Science* 338: 520 – 524
27. Klee CB, Crouch TH, Krinks MH (1979) Calcineurin: a calcium- and calmodulin-binding protein of the nervous system. *Proc Natl Acad Sci USA* 76: 6270 – 6273
28. Saneyoshi T, Kume S, Natsume T, Mikoshiba K (2000) Molecular cloning and expression profile of Xenopus calcineurin A subunit(1). *Biochim Biophys Acta* 1499: 164 – 170
29. Li SJ, Wang J, Ma L, Lu C, Wang J, Wu JW, Wang ZX (2016) Cooperative autoinhibition and multi-level activation mechanisms of calcineurin. *Cell Res* 26: 336 – 349
30. Fujimitsu K, Grimaldi M, Yamano H (2016) Cyclin-dependent kinase 1-dependent activation of APC/C ubiquitin ligase. *Science* 352: 1121 – 1124
31. Qiao R, Weissmann F, Yamaguchi M, Brown NG, VanderLinden R, Imre R, Jarvis MA, Brunner MR, Davidson IF, Litos G, *et al* (2016) Mechanism of APC/CCDC20 activation by mitotic phosphorylation. *Proc Natl Acad Sci USA* 113: E2570 – E2578
32. Zhang S, Chang L, Alfieri C, Zhang Z, Yang J, Maslen S, Skehel M, Barford D (2016) Molecular mechanism of APC/C activation by mitotic phosphorylation. *Nature* 533: 260 – 264
33. Kinoshita E, Kinoshita-Kikuta E, Takiyama K, Koike T (2006) Phosphate-binding tag, a new tool to visualize phosphorylated proteins. *Mol Cell Proteomics* 5: 749 – 757
34. Donella-Deana A, Krinks MH, Ruzzene M, Klee C, Pinna LA (1994) Dephosphorylation of phosphopeptides by calcineurin (protein phosphatase 2B). *Eur J Biochem* 219: 109 – 117
35. Busa WB, Nuccitelli R (1985) An elevated free cytosolic Ca2+ wave follows fertilization in eggs of the frog, Xenopus laevis. *J Cell Biol* 100: 1325 – 1329
36. Goldman A, Roy J, Bodenmiller B, Wanka S, Landry CR, Aebersold R, Cyert MS (2014) The calcineurin signaling network evolves via conserved kinase-phosphatase modules that transcend substrate identity. *Mol Cell* 55: 422 – 435
37. Li H, Zhang L, Rao A, Harrison SC, Hogan PG (2007) Structure of calcineurin in complex with PVIVIT peptide: portrait of a low-affinity signalling interaction. *J Mol Biol* 369: 1296 – 1306
38. Sheftic SR, Page R, Peti W (2016) Investigating the human Calcineurin Interaction Network using the piLxVP SLiM. *Sci Rep* 6: 38920
39. Cao Q, Kim JH, Richter JD (2006) CDK1 and calcineurin regulate Maskin association with eIF4E and translational control of cell cycle progression. *Nat Struct Mol Biol* 13: 1128 – 1134

